2013 American Control Conference (ACC)
Washington, DC, USA, June 17-19, 2013

Enabling Large Load Transitions on Multicylinder Recompression HCCI Engines using Fuel Governors

Shyam Jade, Jacob Larimore, Erik Hellström, Li Jiang, Anna G. Stefanopoulou

***Abstract*— The fuel governor control design methodology presented in [1] is extended and experimentally validated on a multicylinder recompression homogeneous charge compression ignition (HCCI) engine. This strategy regulates desired combustion phasing during load transitions across the HCCI load range. A baseline controller tracks combustion phasing by manipulating valve and fuel injection timings. A reference governor is then added on to the compensated system to modify the fuel injection amount by enforcing actuator constraints.**

Experimental results show improved transient responses of combustion phasing and load during load transitions, when the possibility of constraint violations exists. The nonlinear fuel governor predicts future model trajectories in real-time, and enables larger load transitions than were possible with the baseline controller alone. The complexity and computational overhead of this strategy are reduced by developing a linearized fuel governor, which is shown to work well in the entire HCCI load range and for small variations in engine speed.

I. Introduction

The load range in recompression HCCI engines is bounded from below by high cyclic variability, and from above by constraints on ringing and pressure rise rates [2]. This work aims to design a control strategy that regulates combustion phasing for any load transition in this range.

Auto-ignition timing control in HCCI combustion requires careful regulation of the temperature, pressure and composition of the cylinder charge. Load transitions in HCCI engines are achieved through fuel mass changes, which in turn have a significant effect on charge temperature, and consequently on combustion phasing. These undesired changes in phasing need to be rejected. Large load transients can lead to actuator saturation, in which case the controller authority is lost. This is most pronounced during large load steps down, when reduced temperatures can result in engine misfires, which are unacceptable for emissions and driveability.

Solutions to this problem using optimal control schemes have been proposed, see for example [3]–[5]. However, these involve the on-line solving of a nonlinear optimization problem where the stabilization, tracking and actuator constraint requirements have to be satisfied simultaneously. This problem is simplified through the implementation of the fuel governor, which reduces computation time compared to higher-dimensional optimal control schemes, at the cost of reduced flexibility in shaping the transient response.

Figure 1 shows an overview of the methodology used in this work. Load requirements are converted into desired fuel mass commands (m_f^{des}). A baseline controller uses valve timings and fuel injection timing to track desired combustion phasing (θ_{50}^{ref}). The fuel governor is then added on to the controller-augmented system to improve transient responses during large load transitions. The governor works by attenuating the desired fuel amount change when the possibility of future actuator constraint violations exists.

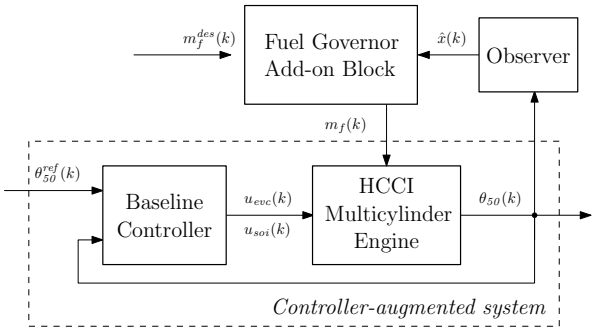

Fig. 1. System overview: The fuel governor is added on to the controller-augmented system. Estimated states are obtained from the observer.

The fuel governor is based on the reference governor concept which separates the closed loop design from the constraint enforcement requirement [6]–[10]. Reference governors have been applied widely in literature, for example to prevent fuel cell oxygen starvation [11]–[13], in hydroelectric power generation [14], [15] and in turbocharged diesel engine supplemental torque control [16].

The paper is structured as follows. The experimental hardware is introduced in Sec. II. A control-oriented model for HCCI combustion is presented, along with validation results. This model is used in Sec. III to develop a baseline combustion phasing controller. The fuel governor is developed in Sec. IV, and is shown to improve phasing and load tracking performance during large load transitions. It enables larger load transitions than were possible with the baseline controller alone. Finally, in Sec. V, the linearized fuel governor is presented, which reduces computational complexity significantly with a minor loss in performance. Validation at different engine speeds demonstrates the efficacy of the approach.

II. HCCI Combustion Modeling

A. Experimental Setup

A four cylinder 2.0 liter GM LNF Ecotec engine running premium grade indolene was used in this study. Modifications to accommodate HCCI combustion include an increased compression ratio of 11.25:1, and shorter duration and lower lift cam profiles to allow for unthrottled operation. In addition

S. Jade, J. Larimore, E. Hellström and A. Stefanopoulou ({sjade, larimore, erikhe, annastef}@umich.edu) are with the Department of Mechanical Engineering at the University of Michigan, Ann Arbor. L. Jiang (li.jiang@us.bosch.com) is with Robert Bosch LLC, Farmington Hills.

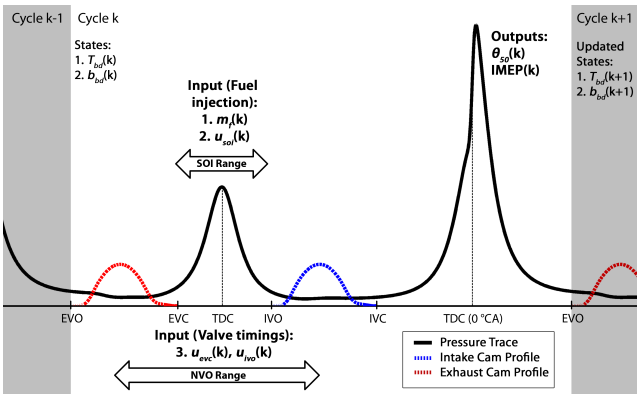

Fig. 2. Typical HCCI in-cylinder pressure trace

to the stock turbo charger an Eaton M24 supercharger was used. Experiments were run at slightly boosted conditions, approximately 1.1 bar intake manifold pressure. Cylinder pressure measurements were used in the ECU to compute combustion phasing in real-time for feedback control.

The control strategies presented in this paper were implemented using a combination of C and Matlab code, and were tested in real-time using an ETAS ES910 rapid prototyping module. The module uses an 800 MHz Freescale PowerQUICC™ III MPC8548 processor with double precision floating point arithmetic and 512 MB of RAM.

B. Control-Oriented Model

The control-oriented model for recompression HCCI combustion is based on work done in [1], [17]. The model has two discrete states, the temperature (T_{bd}) and burned gas fraction (b_{bd}) of the blowdown gases[1]. These states represent thermal and composition dynamics of the system respectively.

As seen in Fig. 2, closing the exhaust valve early and opening the intake valve late causes the characteristic negative valve overlap (NVO) seen in recompression-based HCCI engines [18]. The actuator inputs considered for control, namely the exhaust valve closing timing (u_{evc}), start of fuel injection (u_{soi}), and mass of fuel injected (m_f), affect charge properties in this NVO region. Valve timings are controlled by a hydraulic cam phasing actuator with fixed cam profiles. The intake cam position is fixed. The primary model output is combustion phasing. This is quantified by θ_{50} which is the engine crank angle at which 50% of the total heat release occurs. The work output, represented by the indicated mean effective pressure (IMEP), is a strong function of m_f. In this work, load transitions are represented by fuel mass changes.

1) Model Equations: For a detailed discussion of model structure and equations, please refer to [1], [17]. The key equation in the model is the Arrhenius integral that computes the location of the start of combustion (θ_{soc}). It is given by

$$1 + k_{\text{soi}} u_{soi} = \int_{\theta_{ivc}}^{\theta_{soc}} \frac{A}{\omega} p_c^{n_p} \exp\left(\frac{B}{T_c}\right) d\theta \qquad (1)$$

$$\theta_{50} = \alpha_1 \theta_{soc} + \alpha_0 \qquad (2)$$

[1]The burned gas fraction is the mass fraction of the combustion products excluding excess air. Blowdown is defined after the exhaust valve opens.

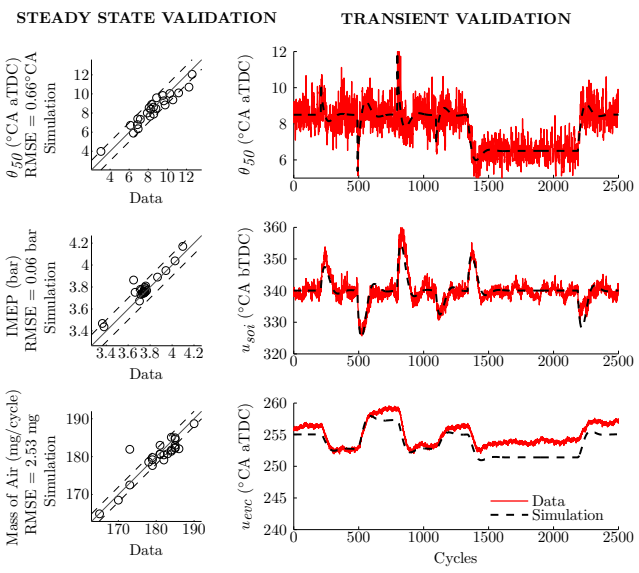

Fig. 3. Steady-state and transient validation results for the model.

TABLE I
LINEARIZATION OPERATION POINT

Quantity (α)	Nominal operating point $(\bar{\alpha})$	Units
u_{evc}	253	°CA aTDC
m_f	10.7	mg/cycle
u_{soi}	330	°CA bTDC
θ_{50}	7.3	°CA aTDC
T_{bd}	870	K
b_{bd}	0.85	-

where θ_{ivc} is the intake valve opening timing, ω is the engine speed, and p_c and T_c are charge pressure and temperatures at angle θ respectively. Here k_{soi}, A, B, n_p, α_i are parameters.

C. Model Validation Results

The control-oriented model was parameterized using steady-state actuator sweep data recorded at an engine speed of 1800 rpm and a boost pressure of 1.1 bar. Figure 3 presents validation results for the model. The plots to the left demonstrate that the steady-state simulated and measured combustion phasing, load and mass of air agree well.

The plots to the right demonstrate satisfactory closed loop model validation. This validation supports the use of the model for predictive model-based control strategies. In these plots, a mid-ranging feedback controller, see Sec. III-A, was implemented both in simulation and on the rapid prototyping hardware. Identical desired load and θ_{50}^{ref} steps were fed to both the model and the engine. The predicted θ_{50}, u_{soi}, and u_{evc} traces match both the magnitude and dynamic behavior of the engine measurements. The u_{evc} drift in Fig. 3 seen after 1500 cycles, is attributed to changing environmental conditions, and does not influence the control strategies presented here, where the prediction horizon is of the order of tens of cycles.

D. Model Linearization

The model is linearized about the operating point in Tab. I. Here $\bar{\alpha}$ is the nominal operating point around which quantity

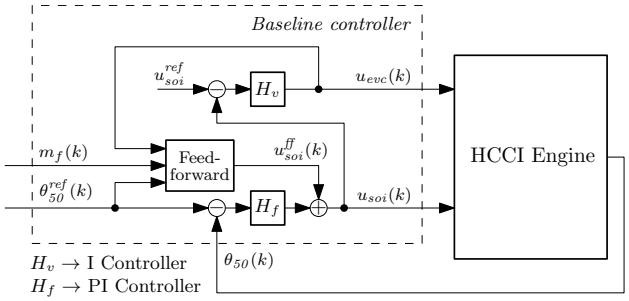

Fig. 4. Baseline Controller: u_{evc} and u_{soi} are in a TISO mid-ranging configuration, with a model-based feedforward component of u_{soi}.

α is linearized.

$$x(k+1) = Ax(k) + Bu(k), \quad y(k) = Cx(k) + Du(k)$$
$$B = [B_{evc}, B_{soi}, B_f], \quad D = [D_{evc}, D_{soi}, D_f]$$
$$x = \left[T_{bd} - \overline{T_{bd}}, b_{bd} - \overline{b_{bd}}\right]^T, \quad y(k) = \theta_{50}(k) - \overline{\theta_{50}}(k)$$
$$u = \left[u_{evc} - \overline{u_{evc}}, u_{soi} - \overline{u_{soi}}, m_f - \overline{m_f}\right]^T \tag{3}$$

where

$$A = \begin{bmatrix} 0.31 & -112 \\ -1.45 \times 10^{-4} & 0.55 \end{bmatrix}, \; C = \begin{bmatrix} -0.096 & 0 \end{bmatrix}$$
$$B_{evc} = \begin{bmatrix} -1.5 \\ 0.004 \end{bmatrix}, B_{soi} = \begin{bmatrix} -0.12 \\ 0 \end{bmatrix}, B_f = \begin{bmatrix} 33 \\ 0.037 \end{bmatrix}$$
$$D_{evc} = 0.47, \; D_{soi} = -0.107, \; D_f = 0.7. \tag{4}$$

This linearized model is used to determine the feedforward component of the u_{soi} control signal in Sec. III-B, and is used to develop the linearized fuel governor in Sec. V.

III. Baseline Controller

The baseline controller in Fig. 1 uses the u_{evc} and u_{soi} actuators to track θ_{50}. As seen in Fig. 4, it comprises of a feedback loop arranged in a mid-ranging control configuration, and a model-based feedforward u_{soi} component.

A. Mid-ranging based Feedback Loop

Mid-ranging is a two-input single-output (TISO) control technique often used in process control [19]. It has also been used in HCCI engine control applications, see for example [20], [21]. This configuration is useful when one actuator provides the required capacity but is slow, while the other actuator is fast but saturates easily. To provide high resolution over the entire operating range, the slow actuator returns the fast actuator to its reference set point at steady state.

In the current application, the u_{evc} and u_{soi} actuators act as the slow and the fast actuators respectively. The u_{evc} actuator has the larger range and greater authority. However, the hydraulic cam phasing actuator is relatively slow, and has a common value for all cylinders. In contrast, u_{soi} saturates easily, but can be set independently from cycle-to-cycle for each cylinder. The θ_{50} tracking error signal drives a PI controller (H_f in Fig. 4) that controls u_{soi}. The slower u_{evc} moves or mid-ranges u_{soi} back towards its reference set point, using an integral controller (H_v in Fig. 4) driven by the u_{soi} tracking error for a reference cylinder, here cylinder 1.

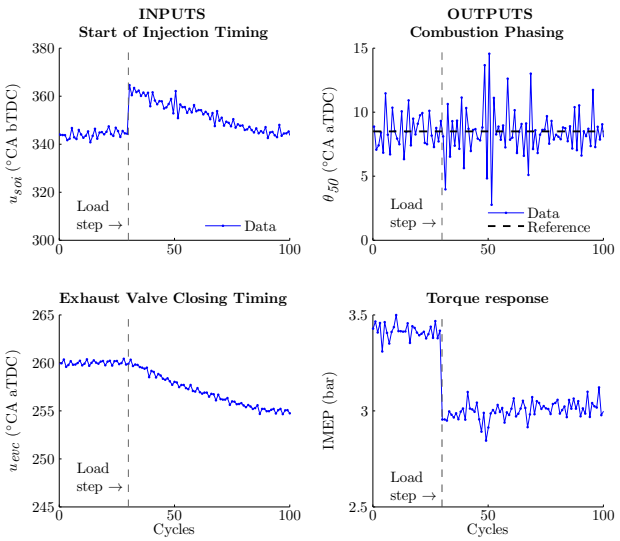

Fig. 5. One cylinder: Baseline controller exhibits reasonable θ_{50} tracking performance for small load transitions ($m_f : 10.5 \rightarrow 8.8$ mg/cycle).

B. Model-based Feedforward

The linearized model in (3) is used to determine the feedforward component of u_{soi}. In Eq. 5, x^{ss} and u_{soi}^{ss} are the steady state states and injection timing input when the linearized system is at steady state, with θ_{50} at θ_{50}^{ref}. Assuming the current values of u_{evc} and m_f to persist at steady state,

$$x^{ss} = Ax^{ss} + B_{soi}u_{soi}^{ss} + B_{evc}u_{evc} + B_f m_f$$
$$\theta_{50}^{ref} = Cx^{ss} + D_{soi}u_{soi}^{ss} + D_{evc}u_{evc} + D_f m_f$$
$$\therefore u_{soi}^{ss} = [0 \quad 1] \begin{bmatrix} (A-I) & B_{soi} \\ C & D_{soi} \end{bmatrix}^{-1} \cdot \begin{bmatrix} -B_{evc} & -B_f & 0 \\ -D_{evc} & -D_f & 1 \end{bmatrix} \begin{bmatrix} u_{evc} & m_f & \theta_{50}^{ref} \end{bmatrix}^T. \tag{5}$$

The feedforward component of u_{soi} is set as u_{soi}^{ss}.

C. Experimental Results

The engine response to a small load step ($m_f : 10.5 \rightarrow 8.8$ mg/cycle) for one cylinder and all cylinders are shown in Fig. 5 and 6 respectively. The combustion phasing controller maintains θ_{50} within reasonable bounds, and the load transitions smoothly between the two set-points. The sudden initial jump in u_{soi} in response to the fuel step is caused by the feedforward component of u_{soi} computed in (5). The u_{evc} actuator slowly mid-ranges the u_{soi} actuator back to its reference set point. Note that the u_{evc} actuator is common for all cylinders, and so the u_{soi} for each cylinder settles to different reference points.

IV. Nonlinear Fuel Governor

Large load transitions result in large changes in the charge temperature. The baseline controller developed in Sec. III is unable to reject the subsequent large variations in θ_{50}. This is seen in Fig. 7, where the baseline controller exhibits poor θ_{50} and IMEP tracking performance after a large load step down ($m_f : 11.4 \rightarrow 8.8$ mg/cycle). The nonlinear fuel governor is developed to improve this poor performance.

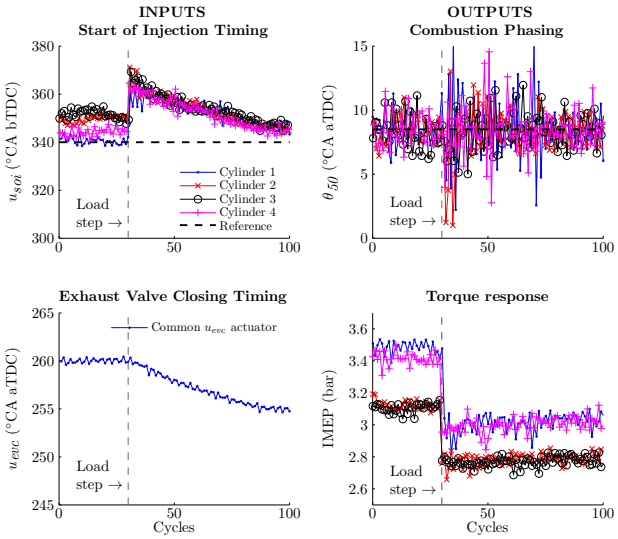

Fig. 6. All cylinders: Baseline controller exhibits reasonable θ_{50} tracking performance for small load transitions (m_f : 10.5 → 8.8 mg/cycle). Note the cylinder-to-cylinder variability in θ_{50} and IMEP.

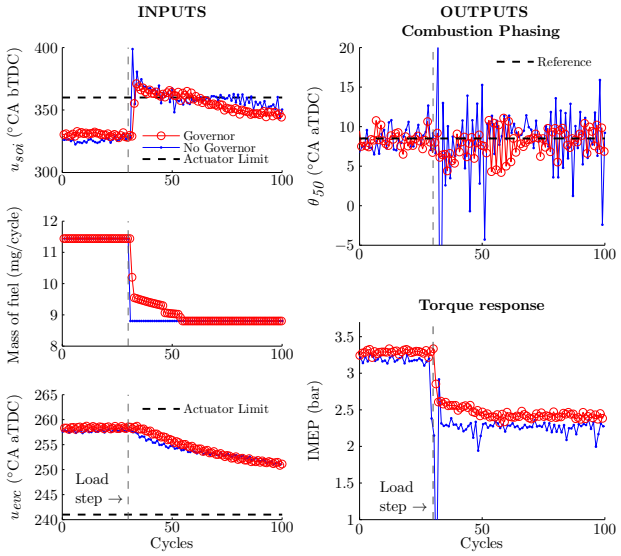

Fig. 7. Use of nonlinear fuel governor improves poor θ_{50} tracking performance for larger load transitions (m_f : 11.4 → 8.8 mg/cycle).

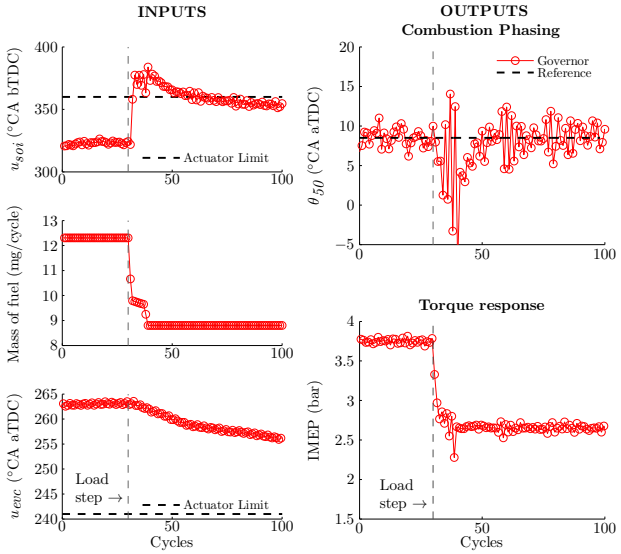

Fig. 8. Use of nonlinear fuel governor allows load transitions that were hitherto impossible (m_f : 12.3 → 8.8 mg/cycle).

As seen in Fig. 1, the fuel governor is added on to the controller-augmented system, and it modifies the desired mass of fuel $(m_f^{des}(k))$ in response to the observed state of the system $(\hat{x}(k))$. The nonlinear fuel governor uses the nonlinear model of the plant, from Sec. II-B, to calculate future trajectories. The fuel governor utilizes the receding horizon principle to check for actuator constraint violation, and is discussed in detail in [1]. Similar to [11], a bisectional search is carried out on the desired change in fuel mass until the optimal value of a single parameter (β) is found:

$$m_f(k) = m_f(k-1) + \beta \cdot (m_f^{des}(k) - m_f(k-1)). \quad (6)$$

Ideally β is set to 1, in which case the fuel governor has no effect, and the desired fuel step is applied unmodified.

At every time step, the system is initialized at the current system states $(\hat{x}(k))$, which are determined from a Luenberger observer designed using the model linearization. The closed loop system is simulated over a fixed future time horizon (N) with the fuel level maintained at $m_f(k)$ calculated in (6). The parameter β is reduced if constraint violations are detected, and is increased if all constraints are satisfied. The optimal value of $\beta \in [0, 1]$ is obtained subject to a convergence tolerance (ϵ). This process ensures that the tracking error between the desired and actual fuel levels is reduced.

The actuator constraints considered in this work are saturation constraints on u_{soi} and u_{evc} and rate constraints on u_{evc}. It was observed that u_{soi} saturation was the only active constraint in experiments, and it was always violated before the u_{evc} constraints. This is a result of the mid-ranging feedback gains chosen for the baseline controller. Note that as long as u_{evc} has authority, u_{soi} will be mid-ranged to the set-point where a feasible solution of $\beta \in [0, 1]$ should exist.

A. Experimental Results

For large load transitions, the fuel governor improves the poor θ_{50} tracking performance exhibited by the baseline controller developed in Sec. III. This is seen in Fig. 7, where the baseline controller alone cannot prevent highly oscillatory θ_{50} and IMEP variations in response to a large load transition (m_f : 11.4 → 8.8 mg/cycle). The fuel governor uses the nonlinear model to predict future constraint violations and slow down the applied fuel mass command. The results in a smaller deviation of u_{soi} from its nominal reference value, and a much smoother transition in θ_{50} and IMEP.

The fuel governor can also extend the load transition range by enabling transitions that would otherwise be impossible to control. By slowing down the m_f command intelligently, an even larger load step down (m_f : 12.3 → 8.8 mg/cycle) in Fig. 8 is successfully negotiated. At the specified boost pressure (1.1 bar) and engine speed (1800 rpm), this load transition spans the entire load range of recompression HCCI.

As seen in Fig. 7 and 8, the governor typically steps m_f

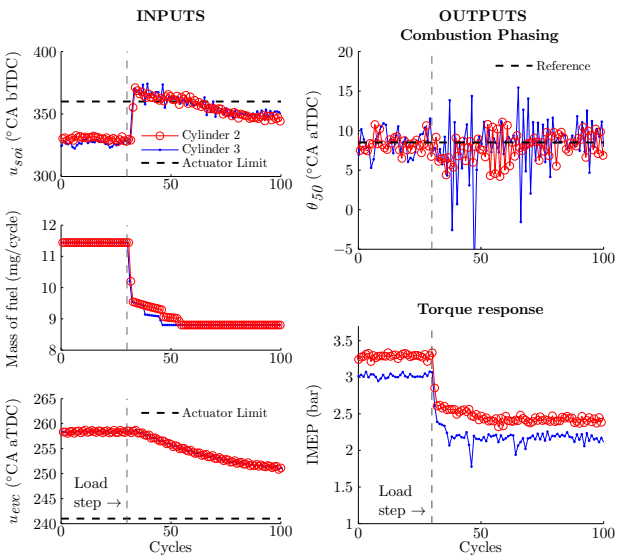

Fig. 9. Potential cylinder-to-cylinder variation after load transition down, caused by cylinder 3 entering a dynamically oscillatory region.

quickly till the u_{soi} constraint is hit. This is followed by a slow relaxation in m_f to its desired value, the rate of which is driven by the u_{evc} response. Note that the u_{soi} constraint has to be made more conservative than the true value. This is done to allow for model and observer errors, and to account for cylinder-to-cylinder variations.

B. Potential Oscillatory Dynamics after Load Step Down

Figure 9 shows the fuel governor response of different cylinders for the same load step down studied in Fig. 7. It illustrates that while the transient response of some cylinders can be excellent, other cylinders sometimes exhibit high cyclic variability in θ_{50}. The initial IMEP and θ_{50} response just after the load transition is satisfactory for both cylinders, which indicates that the fuel governor improves transition performance for all cylinders. However, a few cycles after the load transition, the θ_{50} of cylinder 3 enters an oscillatory region, causing noticeable dips in IMEP.

This behavior is attributed to the baseline controller applying destabilizing control to cylinder 3. As shown in [22], late phasing HCCI combustion dynamics are oscillatory. In these conditions it is important to capture the chemical energy coupling between cycles due to unburned fuel. The onset of the oscillatory dynamics varies with load and with cylinder, as seen in Fig. 9. During the load transition, cylinder 3 entered this oscillatory region while cylinder 2 did not. As seen in [23], gains designed for stable HCCI dynamics are destabilizing when applied in the oscillatory region. Thus the performance gains of the fuel governor will be further improved in future work with a baseline controller that considers the unburned fuel dynamics and globally stabilizes combustion phasing.

V. Realtime Implementation

Implementing real-time predictive control strategies on commercial vehicle-based embedded hardware is challenging due to the computational complexity of optimizing nonlinear models online. Several efforts were made to reduce the complexity and computational runtime of the fuel governor:

1) The nonlinear fuel governor optimizes β in (6) four times every engine cycle. Each optimization requires the nonlinear combustion model to be simulated several times. The number of model simulations per timestep can be reduced by shortening the time horizon (N), and increasing the tolerance (ϵ), as defined in Sec. IV. In this work, $N = 12$ and $\epsilon = 0.05$ were used, to balance performance and computational cost.
2) The Arrhenius integral used to determine the start of combustion, see (1), is computationally very expensive. The integral was replaced with a pre-computed lookup table, based on u_{soi} and T_{bd}.
3) A linearized fuel governor was developed by replacing the nonlinear combustion model with the linear model presented in Sec. II-D.

TABLE II

Comparison of Maximum Runtime for Different Control Strategies for a Standard Series of Load Transitions.

Control Strategy	Maximum Runtime	Normalized Maximum Runtime
Nonlinear Fuel Governor (Arrhenius integral)	8.916 ms	7315%
Nonlinear Fuel Governor (lookup table)	2.315 ms	1900%
Linear Fuel Governor	0.1271 ms	104%
No Fuel Governor	0.1219 ms	100%

Table II shows the typical maximum runtime for different control strategies for a standard series of load transitions. All of the above three strategies were run in real-time on the rapid prototyping hardware described in Sec. II-A. Replacing the Arrhenius integral with a lookup table results in an appreciable runtime improvement. The linearized fuel governor shows a drastic reduction in maximum runtime. The additional computational overhead of augmenting the baseline controller of Sec. III with the linearized fuel governor is only 4%.

A. Linearized Fuel Governor at Different Engine Speeds

The linearized fuel governor is promising from a computational cost perspective. To be able to use this strategy across the entire HCCI load-speed operating range, the nonlinear model has to be linearized at several operating speeds. Each of these linearized fuel governors has to be insensitive to a variation in speeds around its nominal operating point. Figure 10 shows that the linearized fuel governor that is linearized at 1800 rpm performs well for a variation in speeds ($\pm$100 rpm). The linear model is unaware of the speed variation, yet θ_{50} is maintained within reasonable bounds, and IMEP transitions smoothly from one set-point to the another.

VI. Summary and Future Work

The fuel governor controller concept is validated on a multicylinder recompression HCCI engine. The major benefits validated by experiments are improved θ_{50} and IMEP transient

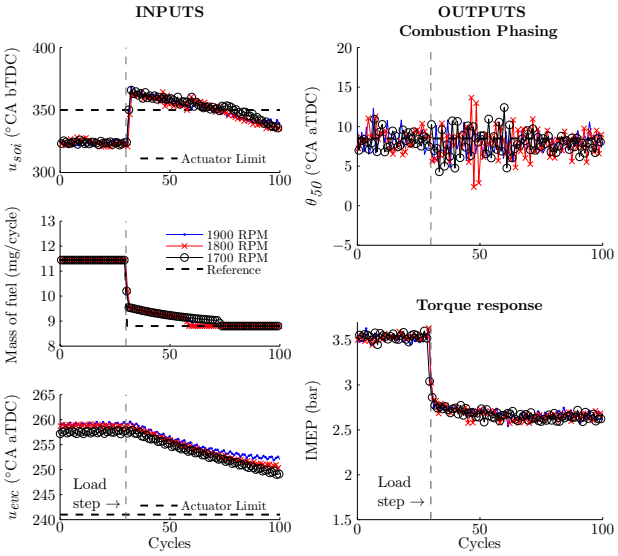

Fig. 10. The linearized fuel governor performs well for a variation of speeds (±100 rpm) around its nominal operating point (1800 rpm).

response during large load transitions (see Fig. 7), and the enabling of larger load transitions than were possible with the baseline controller alone (see Fig. 8). The entire load range at the specified speed and boost pressure can be traversed.

The nonlinear fuel governor is run in real-time on the rapid prototyping hardware. Computational load is reduced significantly by replacing the nonlinear prediction model with a linear model. This linearized fuel governor is proposed as a viable solution for ECU implementation. It is shown to work well in a range of loads and speeds around its nominal linearization operating point (see Fig. 10).

The HCCI model's range of validity is extended to different engine speeds in [24], and will be used in future work to develop controllers for simultaneous load-speed transitions. The range of validity of the linearized fuel governor can be extended across engine speeds by using multiple linearizations. Characterization of the onset of late phasing cyclic variability will be used to improve the performance of the baseline controller in these dynamically oscillatory regions.

Acknowledgments

The authors would like to thank Jeff Sterniak and Julien Vanier of Robert Bosch, LLC for their assistance with troubleshooting experimental issues. This material is supported by the Department of Energy (National Energy Technology Laboratory, DE-EE0003533) as a part of the ACCESS project consortium with direction from Hakan Yilmaz and Oliver Miersch-Wiemers, Robert Bosch, LLC.[2].

[2]Disclaimer: This report was prepared as an account of work sponsored by an agency of the United States Government. Neither the United States Government nor any agency thereof, nor any of their employees, makes any warranty, express or implied, or assumes any legal liability or responsibility for the accuracy, completeness, or usefulness of any information, apparatus, product, or process disclosed, or represents that its use would not infringe privately owned rights. Reference herein to any specific commercial product, process, or service by trade name, trademark, manufacturer, or otherwise does not necessarily constitute or imply its endorsement, recommendation, or favoring by the United States Government or any agency thereof. The views and opinions of authors expressed herein do not necessarily state or reflect those of the United States Government or any agency thereof.

References

[1] S. Jade, E. Hellström, L. Jiang, and A. Stefanopoulou, "Fuel governor augmented control of recompression HCCI combustion during large load transients," in *American Control Conf.*, 2012.

[2] L. Manofsky, J. Vavra, D. Assanis, and A. Babajimopoulos, "Bridging the Gap between HCCI and SI : Spark- Assisted Compression Ignition," *SAE Paper*, no. 2011-01-1179, 2011.

[3] J. Bengtsson, P. Strandh, R. Johansson, P. Tunestål, and B. Johansson, "Model predictive control of Homogeneous Charge Compression Ignition engine dynamics," *IEEE Int. Conf. Control Appl.*, 2006.

[4] C.-J. Chiang and C.-L. Chen, "Constrained control of Homogeneous Charge Compression Ignition (HCCI) engines," *5th IEEE Conf. Ind. Electron. and Appl.*, 2010.

[5] N. Ravi, H.-h. Liao, A. F. Jungkunz, A. Widd, and J. C. Gerdes, "Model predictive control of HCCI using variable valve actuation and fuel injection," *Control Engineering Practice*, vol. 20, pp. 421–430, 2012.

[6] P. Kapasouris, M. Athans, and G. Stein, "Design of Feedback Control Systems for Stable Plants with Saturating Actuators," *Proc. 27th IEEE Conf. Decision and Control*, 1988.

[7] E. G. Gilbert and K. T. Tan, "Linear Systems with State and Control Constraints: The Theory & Application of Maximal Output Admissible Sets," *IEEE Trans. Autom. Control*, vol. 36, pp. 1008–20, 1991.

[8] E. Gilbert, I. Kolmanovsky, and K. Tan, "Discrete-time reference governors and the nonlinear control of systems with state and control constraints," *Int. J. Robust Nonlin. Control*, vol. 5, pp. 487–504, 1995.

[9] A. Casavola and E. Mosca, "Reference governor for constrained uncertain linear systems subject to bounded input disturbances," *35th Conf. on Decision and Control*, 1996.

[10] A. Bemporad, "Reference governor for constrained nonlinear systems," *IEEE Trans. Autom. Control*, vol. 43, no. 3, pp. 415–419, 1998.

[11] J. Sun and I. Kolmanovsky, "Load governor for fuel cell oxygen starvation protection: a robust nonlinear reference governor approach," *IEEE Trans. Control Syst. Technol.*, vol. 13, no. 6, pp. 911–920, 2005.

[12] A. Vahidi, I. Kolmanovsky, and A. Stefanopoulou, "Constraint management in fuel cells : a fast reference governor approach," *American Control Conf.*, 2005.

[13] V. Tsourapas, J. Sun, and A. Stefanopoulou, "Incremental step reference governor for load conditioning of hybrid fuel cell and gas turbine power plants," *American Control Conf.*, 2008.

[14] J. M. Elder, J. T. Boys, and J. L. Woodward, "Integral cycle control of stand-alone generators," *IEE Proc. C - Gener. Transm. Distrib.*, vol. 132, no. 2, pp. 57–66, 1985.

[15] D. Henderson, "An advanced electronic load governor for control of micro hydroelectric generation," *IEEE Trans. Energy Convers.*, vol. 13, no. 3, pp. 300–304, 1998.

[16] I. Kolmanovsky, E. Gilbert, and J. Cook, "Reference governors for supplemental torque source control in turbocharged diesel engines," in *American Control Conf.*, 1997.

[17] S. Jade, E. Hellström, A. Stefanopoulou, and L. Jiang, "On the influence of composition on the thermally-dominant recompression HCCI combustion dynamics," in *ASME Dyn. Syst. Contr. Conf.*, 2011.

[18] J. Willand, R.-G. Nieberding, G. Vent, and C. Enderle, "The knocking syndrome - its cure and its potential," *SAE Paper 982483*, 1998.

[19] B. Allison and A. Isaksson, "Design and performance of mid-ranging controllers," *J. Process Control*, vol. 8, no. 5-6, pp. 469–474, 1998.

[20] M. Karlsson, K. Ekholm, P. Strandh, R. Johansson, P. Tunestål, and B. Johansson, "Closed-loop control of combustion phasing in an HCCI engine using VVA and variable EGR," in *5th IFAC Symp. Advances Auto. Control*, 2007.

[21] N. Ravi, H.-H. Liao, A. F. Jungkunz, and J. C. Gerdes, "Mid-ranging control of a multi-cylinder HCCI engine using split fuel injection and valve timings," *6th IFAC Symp. Advances in Auto. Control*, 2010.

[22] E. Hellström and A. G. Stefanopoulou, "Modeling cyclic dispersion in autoignition combustion," in *IEEE Conf. Dec. Control*, 2011.

[23] H.-H. Liao, N. Ravi, A. Jungkunz, A. Widd, and J. C. Gerdes, "Controlling Combustion Phasing of Recompression HCCI with a Switching Controller," *6th IFAC Symp. Advances Auto. Control*, 2010.

[24] S. Jade, E. Hellström, J. Larimore, A. Stefanopoulou, and L. Jiang, "Reference Governor for Load Control in a Multi-Cylinder Recompression HCCI Engine," *submitted to IEEE Trans. Control Syst. Technol.*